

A SIMPLIFIED ENGINEERING METHOD FOR A T-JOINT WELDING SIMULATION

by

Mato PERIĆ^{a*}, Zdenko TONKOVIĆ^b, Igor KARŠAJ^b, and Dragi STAMENKOVIĆ^c

^a Bureau of Energetics and Mechanical Engineering Ltd., Bestprojekt, Zagreb, Croatia

^b Faculty of Mechanical Engineering and Naval Architecture, University of Zagreb, Zagreb, Croatia

^c IDS Industrieservice Anlagenbau GmbH, Oberhausen, Germany

Original scientific paper

<https://doi.org/10.2298/TSCI171108020P>

In the framework of this study, a hybrid sequential thermo-mechanical finite element analysis of T-joint fillet welding is performed. In the thermal analysis, the element birth and death technique is applied to simulate a weld filler deposition, while a mechanical analysis is performed simultaneously to avoid possible problems due to large displacements induced by large strains. The calculated plate deflections are compared with the experimental measurements while the obtained residual stresses are compared with the analytical solution from the literature. The simulated results demonstrate that the proposed method can be effectively used to predict the residual stresses and distortions induced by the T-joint welding of two plates.

Key words: *welding process, residual stress, T-joint fillet weld, finite element analysis*

Introduction

Fillet welded T-joints have frequently been used in mechanical engineering such as in the vehicle, aircraft, shipbuilding, civil engineering, offshore industries and in many other related fields. The welding of these structures is usually conducted by filler fusion techniques that generate a large amount of heat. Localised heat generation during welding and subsequent rapid cooling lead to the permanent geometrical imperfections of structures and to welding residual stress occurrences [1]. The geometrical imperfections often cause serious problems during assembly while the residual stresses can contribute to fatigue crack initiations, brittle fractures or stress corrosion cracking [2-5]. The elimination of these consequences requires additional financial costs and it is often impossible due to the large structure dimensions.

In recent decades, the progress in rapid computer technology has stimulated many numerical simulation developments and applications to predict the residual stresses and deformations of welded structures in their early design phase [6-10]. Due to frequent application, T-joint fillet welded joints have attracted the attention of many researchers in recent years. Deng *et al.* [11] investigated the influence of plate thickness on welding deformations through experiments and numerical simulations.

The influence of welding sequences on residual stress fields and plate deflections is studied by Gannon *et al.* [12], Lostado *et al.* [13] and Konar *et al.* [14]. Experimental and numerical investigations are carried out by Fu *et al.* [15] to analyse the influence of various factor effects, such as boundary conditions and welding sequences, on residual stress fields and

* Corresponding author, e-mail: mato.peric@fsb.hr

plate deflections. Chen and Soares [16] investigated the effects of plate configurations on weld induced deformations and fillet-welded plate strength. In order to speed the welding simulation process up, Shen and Chen [17], Peric *et al.* [18] and Rong *et al.* [19] proposed novel welding simulation methods based on a combination of shell and 3-D finite elements. Barsoum and Lundback [20] and Wang *et al.* [21] considered gaps and contact between T-joint fillet welded plates. The influence of material property simplifications on temperature fields, residual stress fields and plate deflections in T-joint fillet welded joints are studied by Bhatti *et al.* [22] and Peric *et al.* [23]. Li *et al.* [24] developed an interface element to describe effective penetrations, fillet weld sizes and the contact relationship between plates and stiffeners during welding distortion simulations.

Taking into consideration that the heat generation due to plastic deformation of the material can be neglected in the heat transfer analysis, in all previously mentioned T-joint fillet welding simulations a sequentially-coupled nonlinear computational procedure is used. It means that the computational procedure consists of two independent analyses, *i. e.* thermal and mechanical ones. In the thermal analysis, the transient stress field is calculated using temperature-depending material properties. The obtained thermal history is subsequently used in the mechanical analysis as a thermal load. In both thermal and mechanical analyses, the element birth and death technique is used to simulate weld filler deposition. By using this method, the weld set elements are first deactivated in the thermal analysis and their conductivity is set to a number close to zero. As the heat input is applied, the weld set elements are reactivated and their conductivity is set to the original value. Similarly, in the mechanical analysis, all the weld sets are firstly deactivated and their stiffness is set to a number close to zero. When the elements are reactivated, their stiffness is reset to the original value again. In ABAQUS software, the *MODEL CHANGE option is used to simulate the element birth and death process.

The element birth and death method is used very often because it realistically describes the physical nature of the welding process. On the other hand, it is known that the use of this method can cause serious problems in the mechanical analysis of welding due to large displacements induced by large strains [25]. To overcome these phenomena, a hybrid method is proposed in this study. It means that the element birth and death technique is only used in the thermal analysis to simulate moving heat source. The obtained thermal field is used as a thermal load in the mechanical analysis instantaneously, without the weld filler deposition.

T-joint fillet weld model

To verify the proposed hybrid method, a T-joint fillet weld example from the literature [11] is considered and the geometry and mechanical boundary conditions are given in fig. 1. The welding process is simulated as a single pass, and the welding parameters chosen for this analysis are: CO₂ gas arc welding, welding current $I = 270$ A, welding voltage $U = 29$ V, welding speed $v = 400$ mm/min and a torch angle of $\varphi = 45^\circ$.

The plates are made of carbon steel SM400A and its chemical composition is given in tab. 1. The thermal and mechanical material properties are taken as temperature dependent according to [12] and are presented in figs. 2 and 3. The welds on both sides of the vertical plate are done in a sequence, one after the other, without any time in between. The material is modeled as an elastic-perfectly plastic. In the numerical calculations, it is assumed that the filler and base material have the same thermal and mechanical properties. The influence of phase transformations is not considered in the mechanical analysis because it has an insignificant effect on the residual stresses and deformations in mild steel [26, 27].

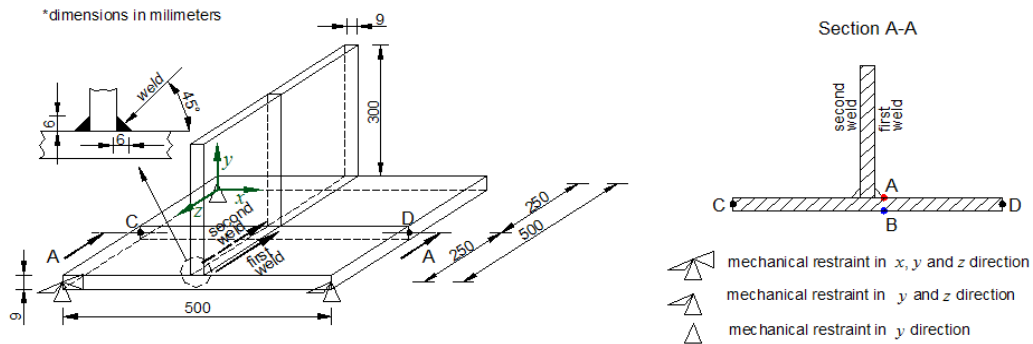


Figure 1. Geometry of T-joint welded plates

The following thermal material properties are assumed: the convective heat transfer coefficient $k = 10 \text{ Wm}^{-2}\text{K}^{-1}$, the efficiency of heat input $\eta = 80\%$ and the surface emissivity factor $\varepsilon = 0.9$. Furthermore, a uniform heat flux distribution per weld volume is used for the heat flux simulation [28, 29], and for this example, the heat flux input is $Q = 5.22 \cdot 10^{10} \text{ Jm}^{-3}\text{s}^{-1}$. To discretize the model geometry, three-dimensional 8-node solid DC3D8 elements are applied in the thermal analysis, and C3D8I elements are used for the mechanical analysis. The same finite element mesh is used in both thermal and mechanical analyses. A typical finite element mesh considered in the present study is shown in Figure 4 and it consists of 19188 finite elements.

Within the framework of the experimental and numerical investigations performed in [11], the middle surface deflection of the horizontal plate along the C-D line seen in fig. 1 is measured and compared with the numerically obtained results. Here, point C is located on the second weld side, while point D is positioned on the first weld side, as presented in fig. 1. Since the experimental measurement of the residual stresses is not performed in [11], the idealised model proposed in [30] is used in the presented study for comparison with the numerically obtained results.

Table 1. Chemical composition of SM400A steel [12]

Chemical composition [mass%]				
C	Si	Mn	P	S
0.23	–	0.56	<0.035	<0.035

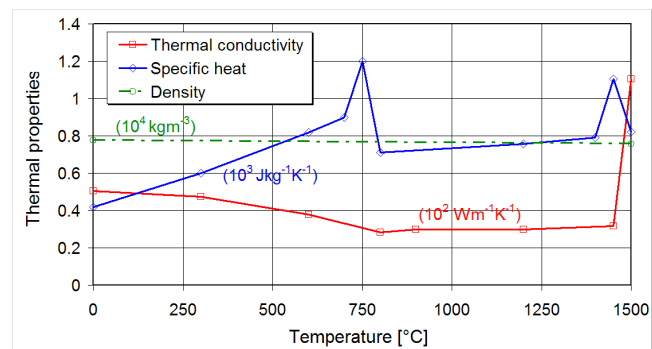


Figure 2. Thermal properties of SM400A steel [12]

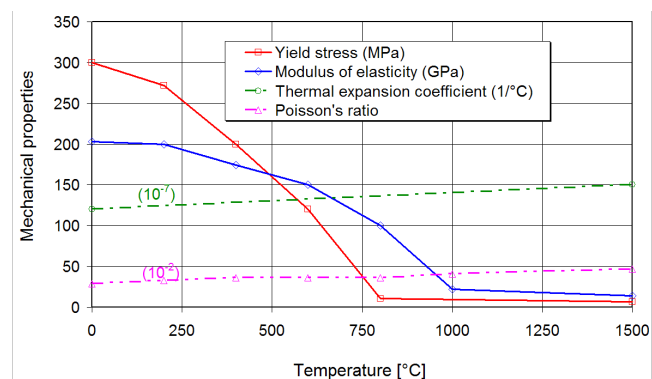


Figure 3. Mechanical properties of SM400A steel [12]

Since the experimental measurement of the residual stresses is not performed in [11], the idealised model proposed in [30] is used in the presented study for comparison with the numerically obtained results.

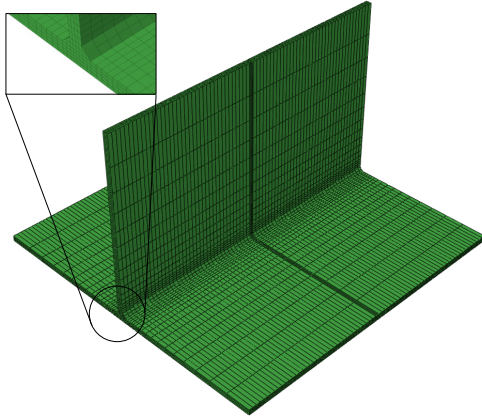


Figure 4. Mesh of finite elements

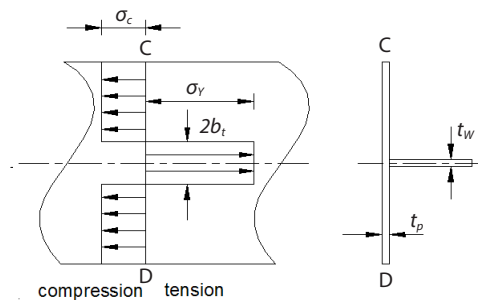


Figure 5. Idealised welding residual stress distribution [30]

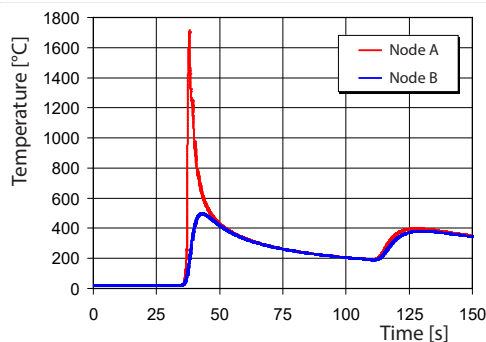


Figure 6. Temperature histories at nodes A and B shown in fig. 1

during the cooling process 50 seconds after the completion of welding as given in fig. 7. The total cooling time to room temperature is about 75 min.

Figure 8 shows the numerically obtained deflection distributions of the horizontal plate at the middle surface along the C-D line shown in fig. 1, after the completion of welding and cooling process. The experimental values obtained by Deng *et al.* [11] are also plotted in the same figure. From this figure, it can be observed that the numerical calculated deflection

This idealised model shown in fig. 5 predicts the residual stress profile in welding direction in the middle surface of the horizontal plate. Here, it is assumed that the highest tensile residual stress is equal to the material yield stress at room temperature, σ_y , while the compressive residual stress in the welding direction, σ_c , can be calculated from the following expression:

$$\sigma_c = \frac{2b_t}{b-2b_t} \sigma_y \quad [\text{MPa}] \quad (1)$$

where b_t is the width of the tensile residual stress zone

$$b_t = \frac{t_w}{2} + \frac{0.26\Delta Q}{t_w + 2t_p} \quad [\text{mm}] \quad (2)$$

$$\Delta Q = 78.8l^2 \quad (3)$$

In eqs. (1) and (2), b represents the horizontal plate width in mm, t_w and t_p are the horizontal and vertical plate thicknesses in mm, while the parameter l is expressed as

$$l = 0.7t_w \text{ when } t_w < 10 \text{ mm}$$

$$l = 7.0 \text{ when } t_w \geq 10 \text{ mm}$$

Results and discussion

The temperature histories at nodes A and B, shown in fig. 1, which are located on the first weld pass side, are presented in fig. 6. The calculated peak temperatures at nodes A and B after the first weld pass are 1712 °C and 496 °C, respectively. This large temperature gradient through the plate thickness causes its bending. After the second weld pass, the temperature gradient between nodes A and B almost disappears as nodes A and B are now far from the heat source. The temperature distribu-

corresponds well with the experimental measurements. The calculated peak deflection is 5.6 mm. The full field of vertical deflection distributions after welding and cooling processes is given in fig. 9.

A comparison of calculated residual stresses in the welding direction along the C-D line (fig. 1) at the middle surface of the horizontal plate with the idealised welding residual distribution is given in fig. 10. The numerically obtained peak tensile residual stresses are approximately 5% higher than the idealised ones. The idealised compressive residual stress obtained from eq. (1) is 48.2 MPa which is very close to the numerical solution at the end of the plates. According to eq. (2), the width of the tensile residual stress zone is 69.2 mm, while the numerical obtained one is 66.3 mm. Finally, it can be concluded that the calculated residual stresses correspond well with the provided idealised solution. The full field residual stress distribution in the welding direction is given in fig. 11. Here, it can be seen that the tensile residual stresses are dominant in the weld and its vicinity while the compressive residual stresses govern the rest of the T-joint.

Conclusions

In this paper, a 3-D hybrid numerical simulation of a T-joint fillet weld is performed to avoid possible problems in the mechanical analysis due to large displacements induced by large strains. In the thermal analysis, the element birth and death method is used to simulate

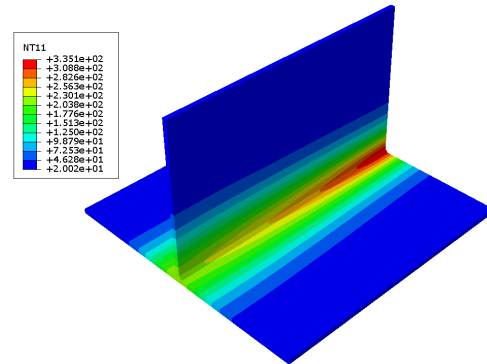


Figure 7. Temperature field distribution 50 second after welding completion (for color image see journal web site)

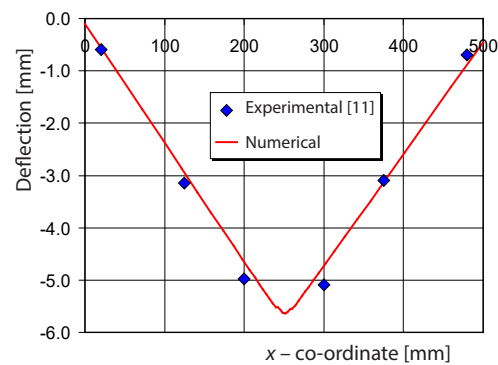


Figure 8. Deflection distributions of horizontal plate at middle surface along C-D line shown in fig. 1

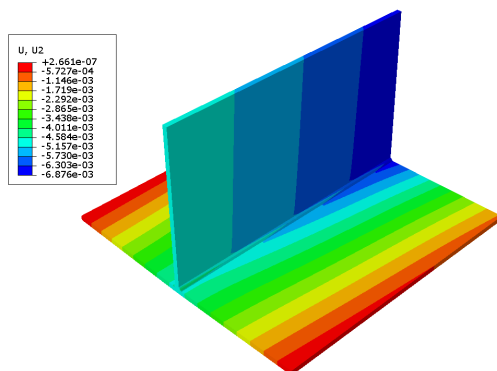


Figure 9. Full vertical deflection field of T-joint welded plates (for color image see journal web site)

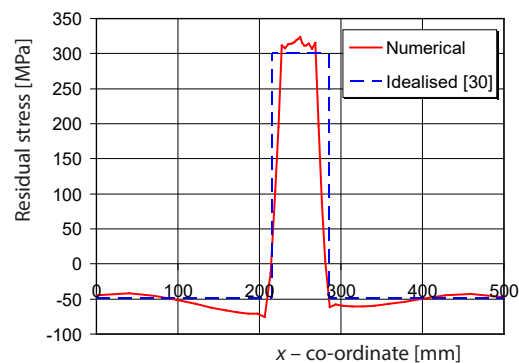


Figure 10. Residual stress in welding direction in middle surface of horizontal plate along C-D line shown in fig. 1

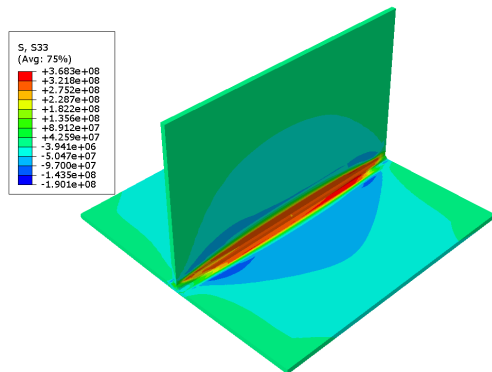


Figure 11. Full residual stress field of T-joint welded plates in welding direction (for color image see journal web site)

the filler metal deposition into the weld pool while the mechanical analysis is done simultaneously, without the filler deposition. The conclusions are as follows.

- The numerically calculated deflections using the hybrid method are in very good correlation with the experimental measurements.
- The numerically obtained residual stresses are very close to the widely used analytical approximation provided in the literature.

As a general conclusion, it can be pointed out that the presented method can be an adequate solution if the problems, due to large displacements induced by large strains in the element birth and death method persist.

Acknowledgment

The herein investigations described are part of the project *Centre of Excellence for Structural Health* (CEEStructHealth) supported by the EU under contract IPA2007/HR/161-PO/001-040513.

References

- [1] Wang, D., et al., Residual Stress Effects on Fatigue Behaviour of Welded T-Joint: A Finite Fracture Mechanics Approach, *Materials and Design*, 91 (2016), Feb., pp. 211-217
- [2] Oh, S. H., et al., Evaluation of J-Groove Weld Residual Stress and Crack Growth Rate of PWSCC in Reactor Pressure Vessel Closure Head, *Journal of Mechanical Science and Technology*, 29 (2015), 3, pp. 1225-1230
- [3] Predan, J., et al., Fatigue Crack Propagation in Threshold Regime under Residual Stresses, *International Journal of Fatigue*, 32 (2010), 7, pp. 1050-1056
- [4] Ding, Y. L., et al., Full-Range S-N Fatigue-Life Evaluation Method for Welded Bridge Structures Considering Hot-Spot and Welding Residual Stress, *Journal of Bridge Engineering*, 21 (2016), 12, pp. 1-10
- [5] Chen, Z., et al., Stress Intensity Factor-Based Prediction of Solidification Crack Growth during Welding of High Strength Steel, *Journal of Materials Processing Technology*, 252 (2018), Feb., pp. 270-278
- [6] Lazić, V. N., et al., Numerical Analysis of Temperature Field During Hard-Facing Process and Comparison with Experimental Results, *Thermal Science*, 18 (2014), 1, pp. 113-120
- [7] Jovičić, G., et al., Residual Life Estimation of a Thermal Power Plant Component: The High Pressure Turbine Housing Case, *Thermal Science*, 13 (2009), 4, pp. 99-106
- [8] Vasović, I. V., et al., Fracture Mechanics Analysis of Damaged Turbine Rotor Discs Using Finite Element Method, *Thermal Science*, 18 (2014), 1, pp. 107-112
- [9] Lostado, R. L., et al., Residual Stresses with Time-Independent Cyclic Plasticity in Finite Element Analysis of Welded Joints, *Metals*, 7 (2017), 4, pp. 1-25
- [10] Aburuga, T. Kh. S., et al., Numerical Aspects for Efficient Welding Computational Mechanics, *Thermal Science*, 17 (2013), 1, pp. 139-148
- [11] Deng, D., et al., Determination of Welding Deformation in Fillet-Welded Joint by Means of Numerical Simulation and Comparison with Experimental Measurements, *Journal of Materials Processing Technology*, 183 (2007), 2-3, pp. 219-225
- [12] Gannon, L., et al., Effect of Welding Sequence on Residual Stress and Distortion in Flat-Bar Stiffened Plates, *Marine Structures*, 23 (2010), 3, pp. 385-404
- [13] Lostado, R. L., et al., Combining Soft Computing Techniques and the Finite Element Method to Design and Optimize Complex Welded Products, *Integrated Computer-Aided Engineering*, 22 (2015), 2, pp. 153-170

- [14] Konar, R., et al., Numerical Simulation of Residual Stresses and Distortions of T-Joint Welding for Bridge Construction Application, *Communications*, 18 (2016), Jan., pp. 75-80
- [15] Fu, G., et al., Effect of Boundary Conditions on Residual Stress and Distortion in T-Joint welds, *Journal of Constructional Steel Research*, 102 (2014), Nov., pp. 121-135
- [16] Chen, B. Q., Guedes Soares, C., Effects of Plate Configurations on the Weld Induced Deformations and Strength of Fillet-Welded plates, *Marine Structures*, 50 (2016), Nov., pp. 243-259
- [17] Shen, J., Chen, Z., Welding Simulation of Fillet Welded Joint Using Shell Elements with Section Integration, *Journal of Materials Processing Technology*, 214 (2014), 11, pp. 2529-2536
- [18] Perić, M., et al., Numerical Analysis and Experimental Investigation in a T-Joint Fillet Weld, *Materials and Design*, 53 (2014), Jan., pp. 1052-1063
- [19] Rong, Y., et al., Study of Welding Distortion and Residual Stress Considering Non-Linear Yield Stress Curves and Multi-Constraint Equations, *Journal of Materials Engineering and Performance*, 25 (2016), 10, pp. 4484-4494
- [20] Barsoum, Z., Lundback, A., Simplified FE Welding Simulation of Fillet Welds – 3-D Effects on Formation Residual Stresses, *Engineering Failure Analysis*, 16 (2009), 7, pp. 2281-2289
- [21] Wang, C., et al., Comparison of FE Models to Predict the Welding Distortion in T-Joint Gas Metal Arc Welding Process, *International Journal of Precision Engineering and Manufacturing*, 15 (2014), 8, pp. 1631-1637
- [22] Bhatti, A. A., et al., Influence of Thermomechanical Material Properties of Different Steel Grades on Welding Residual Stresses and Angular Distortion, *Materials and Design*, 65 (2015), Jan., pp. 878-889
- [23] Perić, M., et al., An Engineering Approach for a T-Joint Fillet Welding Simulation Using Simplified Material Properties, *Ocean Engineering*, 128 (2016), Dec., pp. 13-21
- [24] Li, Y., et al., Prediction of Welding Deformation in Stiffened Structure by Introducing Thermo-Mechanical Interface Element, *Journal of Materials Processing Technology*, 216 (2015), Feb., pp. 440-446
- [25] Safari, A. R., et al., Modeling of Fusion Zone in FE Analysis of the Welding Process, *Journal of Advanced Research in Mechanical Engineering*, 2 (2011), 1, pp. 18-26
- [26] Deng, D., FEM Prediction of Welding Residual Stress and Distortion in Carbon Steel Considering Phase Transformation Effects, *Materials and Design*, 30 (2009), 2, pp. 359-366
- [27] Knoedel, P., et al., Practical Aspects of Welding Residual Stress Simulation, *Journal of Constructional Steel Research*, 132 (2017), May, pp. 83-96
- [28] Perić, M., et al., Comparison of Residual Stresses in Butt-Welded Plates Using Software Packages Abaqus and Ansys, *Scientific Technical Review*, 60 (2010), 3-4, pp. 22-26
- [29] Stamenković, D., Vasovic, I., Finite Element Analysis of Residual Stress in Butt Welding Two Similar Plates, *Scientific Technical Review*, 59 (2009), 1, pp. 57-60
- [30] Yao, T., et al., Ultimate Hull Girder Strength, *Proceedings*, 14th International Ship and Offshore Structures Congress, Nagasaki, Japan, 2000, Vol. 2, pp. 332-333